Prediction of Femoral Impact Forces in Falls on the Hip

Article *in* Journal of Biomechanical Engineering · December 1991

DOI: 10.1115/1.2895414 · Source: PubMed

3 authors, including:

Stephen Robinovitch
Simon Fraser University

Wilson C Hayes
Hayes + Associates, Inc.

Reprinted from November 1991, Vol. 113, Journal of Biomechanical Engineering

S. N. Robinovitch

W. C. Hayes

Orthopedic Biomechanics Laboratory, Department of Orthopedic Surgery, Charles A. Dana Research Institute, Beth Israel Hospital and Harvard Medical School, Boston, MA 02215

T. A. McMahon

Division of Applied Sciences, Harvard University, Cambridge, MA 02138

Prediction of Femoral Impact Forces in Falls on the Hip

A major determinant of the risk of hip fracture in a fall from standing height is the force applied to the femur at impact. This force is determined by the impact velocity of the hip and the effective mass, stiffness, and damping of the body at the moment of contact. We have developed a simple experiment (the pelvis release experiment) to measure the effective stiffness and damping of the body when a step change in force is applied to the lateral aspect of the hip. Results from pelvis release experiments with 14 human subjects suggest that both increased soft tissue thickness over the hip and impacting the ground in a relaxed state can decrease the effective stiffness of the body, and subsequently reduce peak impact forces. Comparison between our fall impact force predictions and in-vitro measures of femoral fracture strength suggest that any fall from standing height producing direct, lateral impact on the greater trochanter can fracture the elderly hip.

Introduction

Falls are the second leading cause of accidental death in the United States, with over 75 percent of all falls occurring in the elderly [22, 23]. In persons over the age of 65, falls represent the leading injury-related cause of death and thus account for the dramatic rise with age in the incidence of injury-related deaths [21]. Beyond these mortality statistics, falls are also associated with significant morbidity, the most important of which is hip fracture. In the United States, about 250,000 hip fractures occur annually among people over the age of 45 [4]. The estimated annual costs of medical and nursing services related to hip fractures is over 7 billion dollars [11, 22]. Moreover, continued growth in the elderly population can be expected to cause the number of hip fractures to rise dramatically, since hip fracture incidence rates increase exponentially with age [16, 19]. If current demographic and incidence trends continue, the annual number of hip fractures may well double or triple by the middle of the next century [12].

Considerable controversy exists regarding whether the majority of hip fractures are disease or accident-related. The steep rise with age in hip fracture incidence, coupled with demonstrated age-dependent reductions in bone density and strength [9, 15, 20, 25], have led to the predominant view that age-related bone loss, or osteoporosis, is the most important determinant of hip fracture incidence [3]. However, others have suggested instead that risk factors for falling are more important [1, 6, 30]. In fact, most densometric indicators of osteoporosis in the proximal femur have failed to differentiate between hip fracture patients and age- and gender-matched controls [5, 7, 25]. On the other hand, in support of the view that hip fractures are primarily related to osteoporosis, it is known that the frequency of hip fracture increases as bone mineral density declines below a densometric fracture threshold in the proximal femur [17, 20, 24]. Faced with these sometimes contradictory results, Melton and Riggs and coworkers [18, 20] have concluded that reduced skeletal resistance to trauma and an increased propensity for falling among the elderly are together important factors for hip fracture risk.

Perhaps the most serious impediment to the design and implementation of intervention efforts aimed at reducing the number of hip fractures is the lack of evidence about what distinguishes injurious from non-injurious falls. While bone strength data are available from experiments on cadaveric femora [2, 8, 13, 14, 26, 27], no previous study has examined the role of fall mechanics in the etiology of hip fracture and therefore we cannot predict whether a given fall will result in fracture. To do so, we must first know the configurations and velocities of the body segments at the moment of impact. We must then be able to use that information to predict the force applied to the hip as a function of time during impact. Finally, we must then compare the predicted hip impact forces with those known to cause hip fracture in vitro.

To address these issues, we have developed a simple experiment (the pelvis release experiment) which allows us to predict potentially injurious fall impact forces based on a lumped-parameter model of body response in low force, zero initial velocity falls on the hip. In addition to providing the estimated force and rate of loading to the impacted hip in a fall, these pelvis release experiments address two hypotheses related to risk factors for hip fracture in a fall: 1) that hip impact forces decrease with increasing amounts of fat covering the hip; and 2) that fall impact forces are significantly decreased when the body contacts the ground in a state of muscle relaxation as opposed to muscle contraction. To explore the first hypothesis, we tested 14 human volunteers of varying body habitus and plotted predicted falling forces against ultrasound measures of soft tissue thickness over the hip. To address the second hypothesis, we examined the difference in impact response of the body in pelvis release experiments arising when a specific protective response (raising the trunk in lateral bending) was inhibited or encouraged. Finally, to evaluate the risk of hip

Contributed by the Bioengineering Division for publication in the JOURNAL OF BIOMECHANICAL ENGINEERING. Manuscript received by the Bioengineering Division August 10, 1990; revised manuscript received March 30, 1991.

Table 1 Subjects

Subject	Gender	Ht.(m)	Wt.(N)	Age	Trochanteric soft tissue thickness (mm)
ATH	Male	1.83	845	24	17
MAM	Male	1.83	742	30	9
MGH	Male	1.75	796	27	26
REB	Male	1.70	618	23	15
SJK	Male	1.70	631	33	15
SJP	Male	1.88	916	21	23
TYT	Male	1.78	760	35	15
ACC	Female	1.60	569	22	27
AEP	Female	1.68	676	25	47
BRM	Female	1.68	542	35	21
DA	Female	1.63	667	21	43
JMD	Female	1.57	693	27	50
MMS	Female	1.73	622	20	29
MSC	Female	1.52	489	34	28

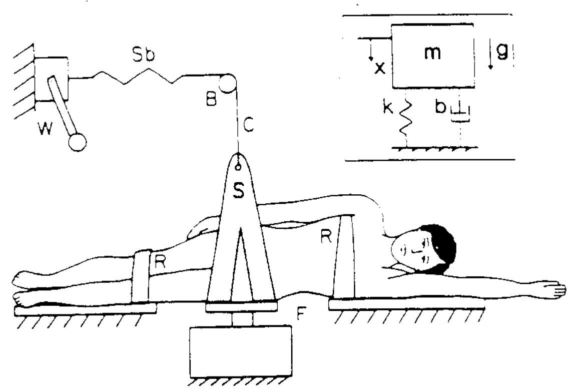

Fig. 1 Apparatus for pelvis release experiments. F: high fidelity force platform; S: pelvis holding sling; R: shoulder and knee restraints; C: steel chain; B: electromagnetic brake; Sb: bias spring; W: winch. The mass-spring-damper model used to simulate the impact response of the body in pelvis release experiments is shown in the inset.

fracture in a fall resulting in direct lateral impact to the hip, we compared pelvis release predictions of fall impact force with previous measures of the force required to fracture the proximal femur in-vitro under load conditions simulating a fall.

Materials and Methods

Subjects and Testing Protocol. A total of seven males and seven females ranging in age from 20 to 35 years and in bodyweight from 489 to 916 N participated in the study (Table 1). To perform a pelvis release experiment, each subject lay with the lateral aspect of the greater trochanter contacting a high-fidelity force platform (natural frequency 101 Hz, measured from impulse response), the lower leg and shoulder resting on platforms, and the pelvis cradled in a canvas sling (Fig. 1). The sling was attached to a steel chain (*C*) which wrapped over a sprocket mounted on an overhead shaft. This shaft could rotate freely or be fixed in place by an electromagnetic brake (model PB-250, Warner Brake Co., Marengo, IL 60152). Before the test began, the investigator manually rotated the shaft, raising the sling to decrease the level of hip reaction force (preload) to a value between 0–500 N, at which point the brake was activated to hold the pelvis in place. Upon release of the brake (measured brake release time 5.5 ms), the level of hip reaction force oscillated about a final level (end load) determined by the preset extension of an extended steel bias spring (Sb). In most pelvis release trials, the bias spring (spring constant 266 N/m) varied less than 3 percent about a mean extension equal to 50 percent of its unstretched length, thereby providing an approximately constant lifting force. Just prior to brake release, the subject was instructed either to completely relax the body (muscle-relaxed) or contract the trunk and back muscles in an atttempt to raise the head and shoulder off the shoulder support (muscle-active). In all trials, an IBM PC/AT computer equipped with Labtech Notebook software (Laboratory Technologies Corporation, Wilmington, MA 01887) was used to acquire hip reaction force data at 150 Hz for a two second period commencing just prior to brake release.

Each subject underwent five muscle-relaxed and five muscle-active pelvis release measures at six predetermined end loads. The parameters obtained from these repeated trials were then averaged to provide representative measures of each subject's response at a given end load. The highest end load was limited to the magnitude of bodyweight resting on the force plate with the bias spring removed (300–600 N, or approximately 2/3 body weight). The lowest end load (approximately 100 N) corresponded to maximum extension of the bias spring. The step input amplitude, or the difference between end load and preload, was approximately constant at 100 N (the lowest step amplitude providing a clear signal) in all tests aside from a series of measures designed to evaluate body response as a function of step input amplitude.

Ultrasound measures of soft tissue thickness over the greater trochanter were acquired in each subject. In these measures, the subject was standing upright, and soft tissue thickness was taken as the distance from the transducer head to the echo from the lateral surface of the greater trochanter.

Several precautions were taken to increase the repeatability of pelvis release measures. Light single-thickness cotton attire was worn by each subject to minimize the effect of clothing on the measured response. Restraining straps at the shoulder and knee ensured consistent body positioning and distribution of weight between the hip, shoulder, and lower leg. Each subject's muscle activity was monitored in all trials through electromyographic (EMG) surface electrodes placed on the spinalis portion of the erector spinae muscle at the level of the tenth rib, the posterior superior portion of the external oblique, and the gluteus medius 5 cm superior to the greater trochanter. These data were acquired and displayed to the investigator with the IBM PC/AT, and displayed to the subject in an oscilloscope placed at eye level. All electrodes were placed on the left side, opposite to that in contact with the force plate.

Mathematical Body Model. The mass-spring-damper model shown in the inset to Fig. 1 is the simplest model capable of simulating the oscillatory response of the body in pelvis release experiments. The mass m, moving with a downward displacement x, strikes the contact surface with a given velocity dx/dt. Energy is absorbed at contact through deflection of a weightless spring of effective stiffness k, and dissipated through a viscous damper of damping coefficient b. The magnitude of m depends on the mass of the pelvis and those portions of the trunk and lower limbs moving with a nonzero downward velocity. The magnitudes of k and b are determined by the force-deflection and force-velocity properties of the soft tissues over the hip, the muscles of the pelvis, abdomen, and lower legs, and the skeletal components themselves.

Including the lifting force of the bias spring (F_S), the equation of motion is

$$m(d^2x/dt^2) + b(dx/dt) + kx = mg - F_S, \tag{1}$$

or

$$(d^2x/dt^2) + 2\zeta\omega_n(dx/dt) + \omega_n^2 x = g - F_S/m, \tag{2}$$

where ω_n is the undamped natural frequency $(k/m)^{1/2}$, ζ is the damping factor $b/(2\omega_n m)$, and g is the gravitational constant, 9.81 m/s^2. Applying initial conditions $x(0) = x_0$ and $dx/dt(0) = u$, and replacing x_0 with F_0/k, where F_0 is the initial force, the solution for x is

$$x = \exp(-\zeta\omega_n t)[A_1\cos(\omega_d t) + A_2\sin(\omega_d t)] + (mg - F_S)/(\omega_n^2 m), \quad (3)$$

where

$$A_1 = (F_0 + F_S - mg)/(\omega_n^2 m) \quad (4)$$

and

$$A_2 = (1/\omega_d)[u + \zeta\omega_n(F_0 + F_S - mg)/(\omega_n^2 m)]. \quad (5)$$

Differentiation of Eq. (3) gives dx/dt, and the force F transmitted to the contact surface is given by

$$F = kx + b(dx/dt). \quad (6)$$

Data Reduction. For each pelvis release trial, an iterative procedure was used to select values of ζ and ω_n best describing the force record throughout the first cycle of vibration. The damping ratio ζ was initially approximated by the logarithmic decrement method as

$$\zeta = (\delta^2/(\pi^2 + \delta^2))^{1/2}, \quad (7)$$

where δ is the logarithmic decrement given by

$$\delta = \ln(x_1/x_2). \quad (8)$$

In Eq. (8), x_1 is the difference between the first force maximum and the end load, and x_2 is the difference between the end load and the first force minimum. The undamped natural frequency ω_n was given by

$$\omega_n = \omega_d/(1 - \zeta^2)^{1/2}, \quad (9)$$

where ω_d is the damped natural frequency $\frac{2\pi}{T_d}$, and T_d is the damped natural period equal to twice the time interval between the first maximum and first minimum in the force record. Since m remained approximately constant for a given body position and state of muscle activity, it was derived from the average end load in the five repeated pelvis release experiments involving zero bias spring tension (note from Eqs. (1) and (6) that the static force level under these conditions equals the effective mass times the gravitational constant). The effective stiffness and damping were then given by

$$k = \omega_n^2 m \quad (10)$$

and

$$b = 2\zeta\omega_n m. \quad (11)$$

A final step in data reduction involved eliminating effects contributed by the finite stiffness of the force platform from measured values of k and b. The methods used in measuring the force platform stiffness are described in Appendix II.

Validation Study. To validate the concept that the force applied to the hip when it strikes the ground with a nonzero initial velocity can be predicted from pelvis release measures of effective stiffness and damping, a mechanical surrogate of the human body was constructed and tested in both zero and nonzero initial velocity drops on the force plate. A comparison was then made between predicted and measured forces in the nonzero initial velocity drops. The methods and results of this experiment are given in Appendix I.

Results

Sample Measures. A number of measures of hip reaction force before, during, and after pelvis release are shown in Fig. 2. In each figure, the solid line represents the measured force and the dotted line represents the simulated force given by Eq. (6). Figures 2(*a*) and (*b*) show the measured response of a 667 N, 21 year old female subject (DA) in the muscle-relaxed state. In the first trial, the preload was 15 N and the end load 93 N. In the second trial, a decrease in bias spring tension increased the force levels to 323 and 407 N, respectively. Since body position and muscle activity did not vary between the two trials, m remained constant (40 kg). However, increasing the end

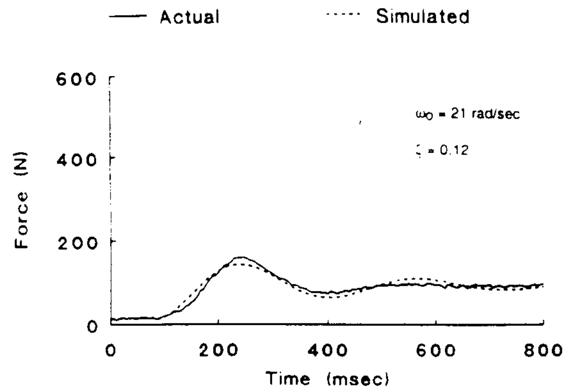

Fig. 2(*a*)

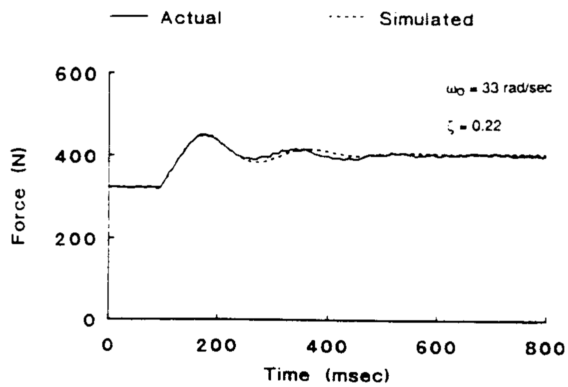

Fig. 2(*b*)

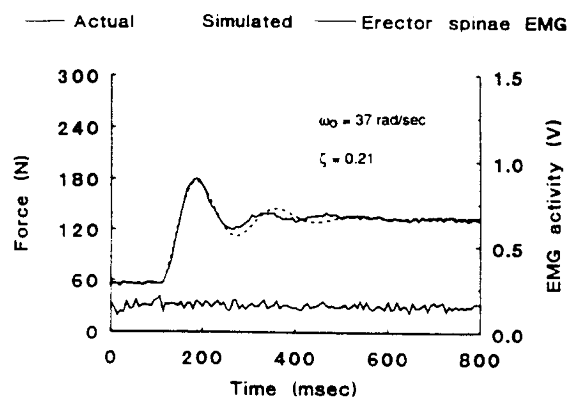

Fig. 2(*c*)

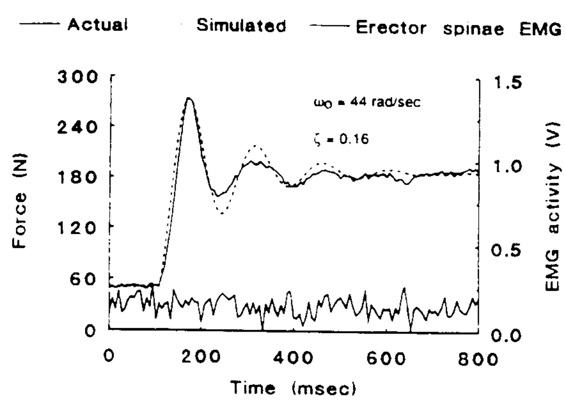

Fig. 2(*d*)

Fig. 2 Results of four pelvis release experiments showing the effects of end load and muscle contraction on the observed response: (*a*) female subject (DA) in low end load, muscle-relaxed measure; (*b*) female subject (DA) in high end load, muscle-relaxed measure; (*c*) male subject (REB) in medium end load, muscle-relaxed measure; (*d*) male subject (REB) in medium end load, muscle-active measure. The solid curves give measured results; the broken curves show the predictions of Eq. (6).

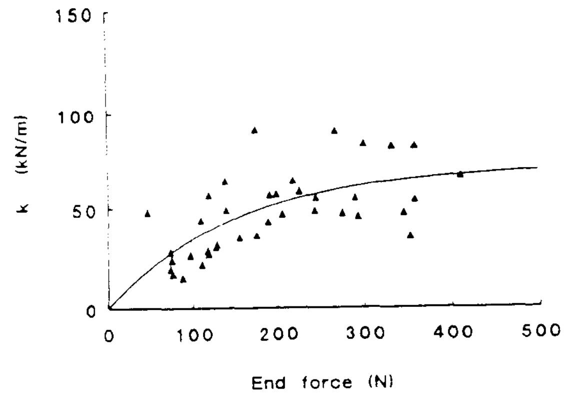

Fig. 3(*a*)

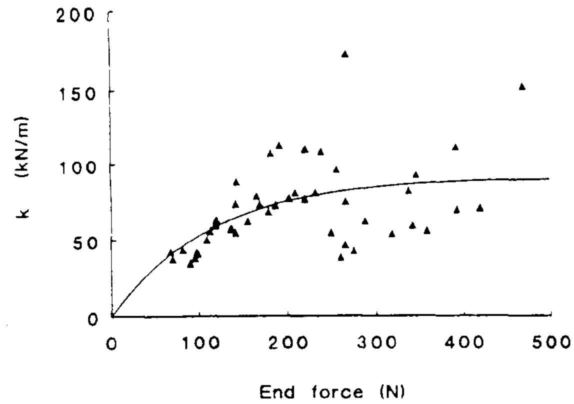

Fig. 4(*a*)

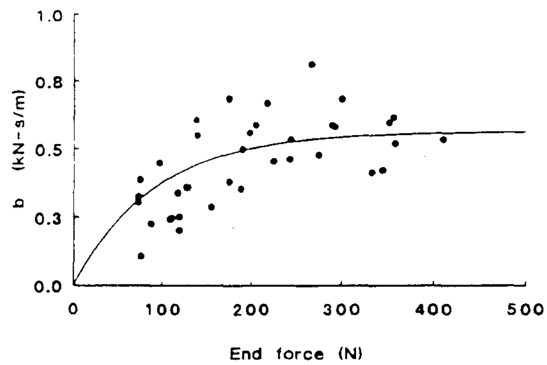

Fig. 3(*b*)

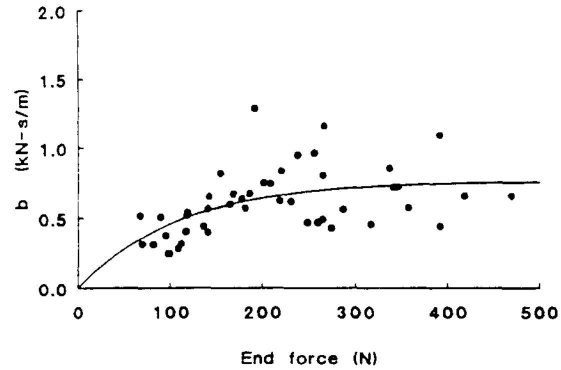

Fig. 4(*b*)

Fig. 3 Effect of end load on (*a*) effective stiffness *k* and (*b*) effective damping *b* for female subjects. Exponential curves show typical subject behavior. Note that both *k* and *b* plateau above end loads of 250 N.

Fig. 4 Effect of end load on (*a*) effective stiffness *k* and (*b*) effective damping *b* for male subjects. Exponential curves show typical subject behavior. Note that both parameters plateau beyond end loads of 200 N.

load caused increases in both ω_n (57 percent from 21 to 33 rad/s) and ζ (83 percent from 0.12 to 0.22). Corresponding rises occurred in both k (146 percent from 17.7 to 43.6 kN/m) and b (188 percent from 201 to 580 N-s/m). Figures 2(*c*) and (*d*) show the measured response of a 618 N, 23 year old male (REB) in both muscle-relaxed and muscle-active states. It is apparent that erector spinae EMG activity increased considerably in the muscle-active case. Furthermore, muscle contraction caused significant increases in m (58 percent from 31 to 49 kg), k (116 percent from 44.2 to 95.6 kN/m), and b (40 percent from 506 to 709 N-s/m). It is interesting to note that b increased in the muscle-active state despite the fact that ζ decreased.

Estimates of Nonlinear Stiffness and Damping. Pelvis release experiments measured the response of the body to small step inputs in force (approximately 100 N). Each trial therefore characterized k and b for a given level of force, or end load. However, since these parameters generally increased with increasing end load, the response of the body to high amplitude inputs in force, such as those occurring in actual falls, will be nonlinear. To incorporate this nonlinear behavior into our model of impact response, a least-squares method was utilized to derive exponential functions describing the variation in k and b with end load. Regressions were performed on data from each subject and on data combined from all subjects but separated by sex.

The stiffening nature of the body spring and damper was best described by an exponential function with zero magnitude at zero end load, increasing to a constant level at high end load. In the muscle-relaxed state, both female (Figs. 3(*a*) and (*b*)) and male (Figs. 4(*a*) and (*b*)) values of k and b plateaued well within the experimental range of end load (200–300 N). In the muscle-active state (not shown), female values of k and b again plateaued in the high range of end load, but male parameters continued to increase through the entire range of end load. Best-fit exponential functions of muscle-relaxed data, along with corresponding coefficients of determination (R^2), were given for females as

$$k = 71{,}060(1-\exp(-F/151));\ (R^2 = 0.415), \qquad (12)$$

$$b = 561(1-\exp(-F/91));\ (R^2 = 0.208), \qquad (13)$$

and males as

$$k = 90{,}440(1-\exp(-F/114));\ (R^2 = 0.222), \qquad (14)$$

$$b = 756(1-\exp(-F/108));\ (R^2 = 0.233), \qquad (15)$$

where F is force in N, k is stiffness in N/m, and b is the damping coefficient in N-s/m. Note that between-subject differences in body habitus caused a considerable scatter in k and b with end load.

In an effort to assess the repeatability of pelvis release experiments, three subjects returned for a second test session one week after the initial session. In measures taken at end loads of 100 and 300 N, average between-session changes in k and b were 11.3 and 17.5 percent, respectively. There was no discernible pattern to the changes; k and b neither increased nor decreased consistently from one week to the next. Within-session repeatability was reflected by sample standard deviations in the five repeated measures taken at each force level, which averaged 15 and 17 percent of the mean for k and b, respectively.

The effect of step input amplitude on the impact response

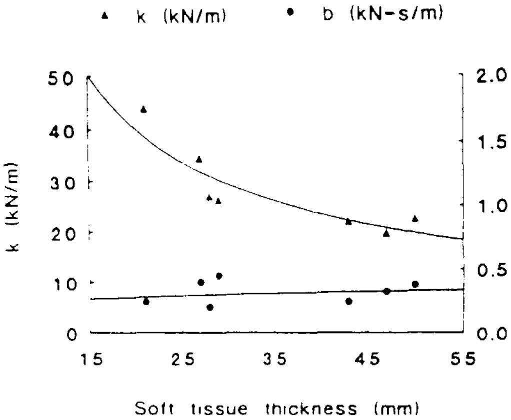

Fig. 5(*a*)

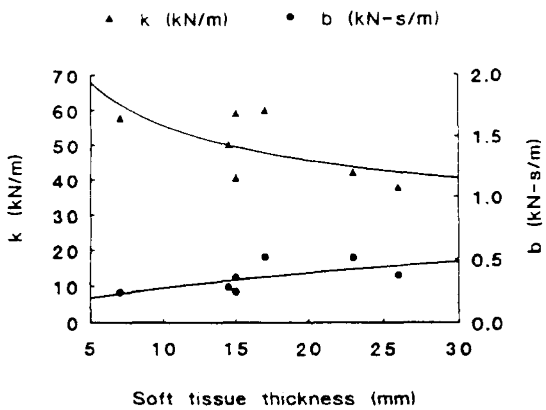

Fig. 5(*b*)

Fig. 5 Effect of trochanteric soft tissue thickness on the magnitudes of *k* and *b* at 100 N end load for (*a*) females and (*b*) males. Females showed negative correlation between *k* and soft tissue ($R^2 = 0.828$), but little if any correlation between *b* and soft tissue thickness ($R^2 = 0.0378$). Males showed moderate negative correlation between *k* and soft tissue thickness ($R^2 = 0.387$), and moderate positive correlation between *b* and soft tissue thickness ($R^2 = 0.456$).

of the body was evaluated in three individuals who underwent pelvis release tests in which the preload was varied while a constant end load of 400 N was maintained. These data showed that, for a range of amplitude between 100–240 N, values of k and b increased with amplitude, rising 22 and 20 percent, respectively, as the amplitude rose 140 percent. Greater nonlinearity was observed in late periods of ringing in the high amplitude tests, perhaps reflecting the occurrence of a reflex-based protective response.

Effect of Soft Tissue Thickness and Muscle Activation. Figures 5(*a*) and (*b*) show the effect of trochanteric soft tissue thickness on average values of k and b at 100 N end load. Least-squares fits of power functions to female data revealed a negative correlation ($R^2 = 0.828$) between k and soft tissue thickness, but little if any correlation between b and tissue thickness ($R^2 = 0.0378$). Males exhibited moderate negative correlation between soft tissue thickness and both k ($R^2 = 0.387$) and b ($R^2 = 0.456$), perhaps due to the low mean and between-subject variation in male trochanteric soft tissue (Table 1).

In both males and females, transition into the muscle-active state caused increases in the average values of m (26 percent from 35 to 44 kg), k (86 percent from 58 to 108 kN/m), and b (46 percent from 515 to 754 N-s/m). Such changes were especially noticeable in males of low body fat, who were perhaps able to achieve a higher state of muscular contraction, and subsequently greater effective stiffness and damping.

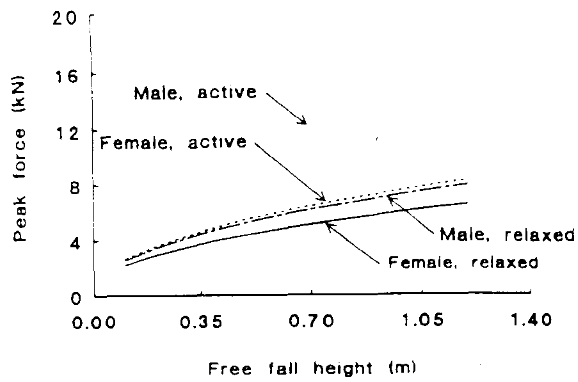

Fig. 6(*a*)

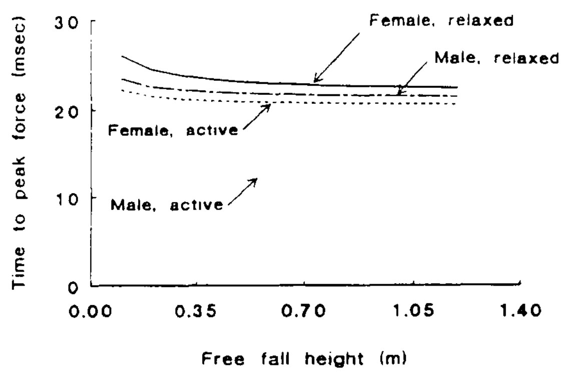

Fig. 6(*b*)

Fig. 6 Effect of drop height, gender, and muscle activity on (*a*) predicted peak impact force and (*b*) rise time to peak force. Peak forces were higher in males than females, and higher in the muscle-active than muscle-relaxed state. Rise times to peak force were lower in males than females, and lower in the muscle-active than muscle-relaxed state.

Predicted Force-Time History in Nonzero Height Falls. In order to estimate the typical force applied to the proximal femur in falls in both muscle-relaxed and active states, average values of the effective pelvis release mass m and exponential functions describing the variation in k and b with force (shown for the muscle-relaxed state in Eqs. (12)–(15)) were incorporated into Eqs. (2) and (6). A fourth order Runge-Kutta numerical integration technique was then utilized to solve Eq. (2) based on initial conditions $x(0) = 0$ and $dx/dt(0) = u$, where u was given by consideration of free-fall of the effective mass from an initial height h:

$$u = (2gh)^{1/2}. \tag{16}$$

The simulated fall therefore involves initiation of the descent phase from height h, ground contact of the arm and lower leg, and finally contact of the hip. Note, however, that contact of the arm and lower leg does not act to decrease pelvis velocity. This initial contact acts only to reduce the effective (moving) mass to the value m measured in pelvis release experiments. For males, this value averaged 39 kg in the muscle-relaxed state and 49 kg in the muscle-active state. In females, m averaged 31 kg in the muscle-relaxed state and 37.6 kg in the muscle-active state.

The predicted peak forces (F_{max}) and rise times to peak force are displayed as functions of h in Figs. 6(*a*) and (*b*). Note that changes in m, k, and b caused F_{max} and rise time to peak force to change considerably between males and females and between muscle-relaxed and active states. Specifically, the following observations can be made: 1) males showed larger values of

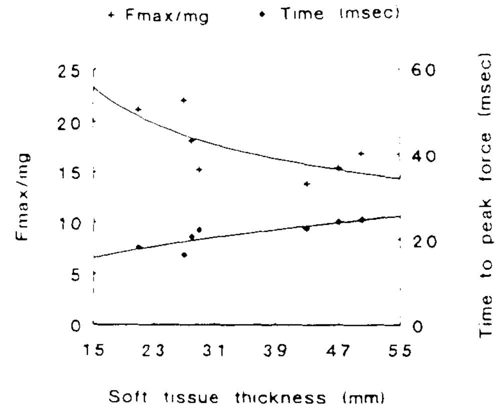

Fig. 7(a)

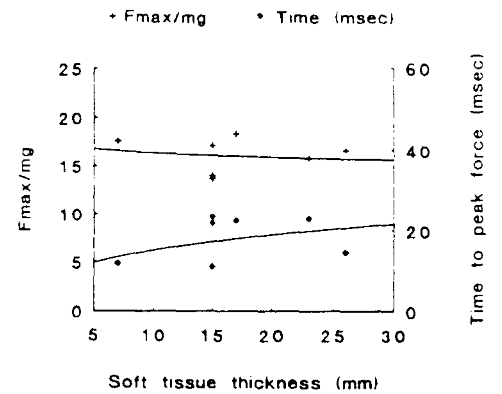

Fig. 7(b)

Fig. 7 Effect of trochanteric soft tissue thickness on the nondimensional parameter F_{max}/mg and rise time to peak force in (*a*) females and (*b*) males. Females showed negative correlation between F_{max}/mg and soft tissue thickness ($R^2 = 0.500$), and positive correlation between rise time to peak force and soft tissue thickness ($R^2 = 0.644$). Males showed little if any correlation between soft tissue thickness and F_{max}/mg ($R^2 = 0.0231$) or rise to peak force ($R^2 = 0.201$).

m and k than females, and subsequently male values of F_{max} were larger than female (21 percent in the muscle-relaxed state, 91 percent higher in the muscle-active state); 2) males showed larger values of b and k than females, and subsequently male rise times to peak force were lower than female (24 percent lower in the muscle-relaxed state, 41 percent lower in the muscle-active state); 3) increased m and k in the muscle-active state caused muscle-active values of F_{max} to average 66 percent higher than muscle-relaxed; 4) increased b and k in the muscle-active state caused muscle-active rise times to peak force to average 24 percent lower than muscle-relaxed.

In order to examine the effect of soft tissue thickness on predicted impact forces in muscle-relaxed falls, numerical integrations of Eq. (2) were performed based on values of m and exponential regressions of k and b for each subject. In these simulations, the contact velocity was held constant at 3.7 m/s, corresponding to initiation of the fall from a pelvis height of 0.7 m. The resulting normalized peak force F_{max}/mg (where mg is the effective pelvis release weight) and rise time to peak force are displayed as functions of soft tissue thickness in Figs. 7(*a*) and (*b*). It can be seen that females exhibited negative correlation between tissue thickness and F_{max}/mg ($R^2 = 0.500$), and positive correlation between tissue thickness and time to peak force ($R^2 = 0.664$). However, males demonstrated little if any correlation between tissue thickness and F_{max}/mg ($R^2 = 0.0231$) or rise time to peak force ($R^2 = 0.210$), again perhaps due to the lack of obese male subjects in our study.

Discussion

There are three important limitations to our study. First, the young age of the human subjects in this study may limit the applicability of the conclusions to elderly populations who are at greatest risk of falling. Specifically, age-related changes in height, body weight, muscle strength, and soft tissue thickness over the hip may be responsible for falling forces significantly different from those predicted here. Second, pelvis release experiments measured the force transmitted from the force platform to an area formed not only by the soft tissue overlying the proximal femur, but also portions of the ilium and the proximal femoral diaphysis. While the small size of the contact area and the central position of the greater trochanter ensured that the majority of this load was directed to the proximal femur, at this point we cannot completely characterize the distribution of force throughout the impacting surface. Lastly, our analysis was restricted to a special fall case in which the lateral aspect of the hip impacts the ground after the arm and knee. The results may therefore have limited application to falls when impact occurs to the anterior or posterior aspect of the pelvis, or when the hand does not strike the substrate before the hip. Previous research has shown most fallers who fracture their hip fall to the side, land directly on the hip, and do not use the outstretched hand to break the fall [10]. Therefore, while our fall simulation may represent a severe case, many falls occur which present even greater risks for hip fracture.

Two additional points regarding the simulated fall should be considered. First, while the posture of Fig. 1 was experimentally convenient, no evidence exists that it represents a common fall impact configuration. Second, although we neglected the potential decrease in hip impact velocity caused by initial contact with the leg or outstretched hand, Eq. (16) and Fig. 6 together provide a means for estimating fall severity for any value of hip impact velocity between 1.2–4.8 m/s.

In this study, we developed and applied a method for predicting the force applied to the proximal femur in falls from standing height. Three important conclusions arose from the results: 1) the method appears to represent a useful technique for characterizing the peak force and rate of loading to the impacted hip in a fall; 2) the experimental results appear to confirm our hypothesis that fall impact force attenuation is directly related to the thickness of soft tissue over the hip; and 3) the results also support our second hypothesis, that fall impact forces should be reduced significantly by striking the ground in a relaxed state.

While ethical considerations prevented the use of human subjects to verify the fall force predictions of the mass-spring-damper model, the utility of the method was confirmed by validation tests with the human body surrogate (Appendix I). First, the spring stiffness measured in dynamic tests similar to pelvis release experiments closely matched that measured in static force-deflection tests. Second, the model successfully predicted loading under conditions involving threefold increases in peak forces above those used in the trials formulating the model. Although the surrogate consisted of linear springs and dashpots, while corresponding elements in the human body are nonlinear, we measured these nonlinear elements as functions of force in human subjects and incorporated the resulting nonlinear correlations in our human body model. Therefore, unless an actual fall causes a discontinuity at high force levels in our functions describing the measured variation of k and b with end load (which may result from trauma to a bone or ligament, but is otherwise unlikely), we can propose no reason why our human fall force predictions should not estimate the peak force in a fall nearly as well as our validating tests with the human body surrogate.

In female subjects, threefold increases in trochanteric soft tissue thickness caused 57 percent reductions in effective stiffness and 34 percent reductions in fall impact force. Based on these observations and the known nonlinear force-deflection properties of soft tissue [29, 31], we propose the soft tissue overlying the hip can be described by a rounded surface with an infinite number of springs and dampers in parallel. At the moment of impact, the small contact area between the hip and the ground causes the effective stiffness and damping of the body to be small. As the contact area increases, more springs and dampers compress. Eventually, a stiffening of the soft tissue occurs (this stiffening will occur at lower force levels in individuals with low soft tissue thickness), at which point the stiffness and damping of the underlying bone begin to contribute significantly to k and b. This model is consistent with our functional representations of k and b, which had zero magnitude at zero end load and approached constant values at high end load.

Results of this study suggest the state of muscle activity at impact may be a more important determinant of fall fracture risk than soft tissue thickness over the hip. For example, muscle activation in males caused 100 percent increases in predicted average peak force, and 43 percent decreases in rise times to peak force. These changes reflect two phenomena caused by contraction of the trunk muscles at impact: 1) a shift in support of the body weight from the upper extremity to the hip, and subsequent increases in m; and 2) an increase in the rigidity of muscular connections between the trunk, pelvis, and lower limbs, and subsequent increases in m, b, and k. Therefore, while neuromuscular control in the descent phase of the fall may reduce the velocity of impact and allow the faller to adjust the body into a safe landing configuration, striking the ground in a stiff state actually increases impact force.

A recent study by Viano [28] measuring cadaveric response to blunt lateral impact provides data which may be compared to our force predictions. In Viano's study, six male and two female cadavers were impacted on the lateral aspects of the greater trochanter with a 23.4 kg pendulum of 15 cm surface diameter. Peak contact forces and pelvic deflections were found to average 5.45 kN and 4.9 cm for an average impact velocity of 4.83 m/s, 6.81 kN and 9.85 cm for an average impact velocity of 6.77 m/s, and 11.2 kN and 7.83 cm for an average impact velocity of 9.65 m/s. We simulated this experiment as two masses (one mass being the initially moving 23.4 kg pendulum, the other being the initially stationary effective body mass) separated by a parallel spring/damper combination identical to that measured in pelvis release experiments. Using average muscle-relaxed male data for effective body stiffness, damping (Eqs. (14)–(15)), and mass (39 kg), we predicted peak forces and deflections of 4.57 kN and 3.4 cm for an impact velocity of 4.83 m/s, 6.40 kN and 4.76 cm for an impact velocity of 6.77 m/s, and 9.20 kN and 6.79 cm for an impact velocity of 9.65 m/s. Viano's measured time to peak force averaged approximately 10 ms in the low velocity impacts and 6 ms in the high velocity impacts, while in all of our simulations the time to peak force was approximately constant at 7.6 ms. Our simulation therefore provides reasonably good predictions of the measured response in terms of peak force, rate of load, and peak deflection.

In order to compare the fall impact force predictions of our study with the measured in vitro fracture strength of the proximal femur, consider an average individual falling from a 0.7 m height and landing in a position duplicating the body configuration of the pelvis release experiments. Taking the average of male and female values, our results predict that such an individual experiences peak hip impact forces of approximately 5600 N falling in the muscle-relaxed state, and 8600 N falling in the muscle-active state. The position of the body causes this load to be applied to the lateral aspect of the greater trochanter, oriented directly toward the opposite greater trochanter.

Two previous studies have measured the in vitro fracture strength of the proximal femur in simulated fall loading configurations. Lotz and Hayes [14] applied a quasi-static load to the posteriolateral aspect of the greater trochanter, simulating a fall with the leg raised 30 degrees and the load directed 30 degrees posterior to the plane formed by the neck and diaphysial axes. Measured fracture forces ranged from 778 to 4093 N. Smith [27] applied a dynamic load to the lateral aspect of the greater trochanter, orienting the load vector in the horizontal plane and the plane formed by the neck and diaphysial axes. Reported fracture forces were significantly higher (2668 to 15034 N), probably because Smith loaded the femoral neck against its strong axis, while Lotz and Hayes oriented the load toward the weak axis. While no data are available for the loading configuration of pelvis release experiments (a loading in the frontal plane, approximately 15 degrees posterior to the strong axis of the femoral neck), it is apparent that our peak force predictions are significantly greater than fracture forces reported by Lotz and Hayes, and well within the range of those of Smith.

In summary, we have developed a method of predicting the load applied to the hip at impact following a fall. This method can be used to evaluate the relative risk of hip fracture associated with different kinematic states of the body at contact. Current results show that both soft tissue compression and muscle relaxation may significantly reduce impact forces. However, comparison of our force predictions with previous in-vitro femoral fracture strength measures suggests that, even in the least severe case of females falling in the muscle-relaxed condition, a fall to the side producing lateral impact on the greater trochanter has the potential to fracture an elderly hip every time it happens.

Acknowledgments

This study was supported by grants from the Center for Disease Control (CR 102550), the New England Injury Prevention Research Center (R49 CCR103605), and by the Maurice E. Mueller Professorship of Biomechanics at the Harvard Medical School (WCH). The authors wish to thank Dr. Toshitsugu Takeuchi for his assistance in electromyography.

References

1 Aitken, J. M., "Relevance of Osteoporosis in Women with Fractures of the Femoral Neck," *Br Med J.*, Vol. 288, 1984, pp. 597–601.

2 Alho, A., Husby, T., and Hoiseth, A., "Bone Mineral Content and Mechanical Strength. An ex-vivo Study of Human Femora at Autopsy," *Clin Orthop Rel Res*, Vol. 227, 1988, pp. 292–297.

3 Anonymous, "Consensus Conference: Osteoporosis," *JAMA*, Vol. 252, 1984, pp. 799–802.

4 Anonymous, "National Center for Health Statistics. Advance Data from Vital and Health Statistics: 1985 Summary: National Hospital Discharge Survey," Hyattsville, MD, 1986, PHS 86–1250.

5 Bohr, H., and Schaadt, O., "Bone Mineral Content of Femoral Bone and Lumbar Spine Measured in Women with Fracture of the Femoral Neck by Dual Photon Absorptiometry," *Clin Orthop Rel Res*, Vol. 179, 1983, pp. 240–245.

6 Cummings, S. R., "Are Patients with Hip Fractures More Osteoporotic?" *Am J Med*, Vol. 78, 1985, pp. 487–493.

7 Eriksson, S. A. V., and Widhe, T. L., "Bone Mass in Women with Hip Fracture," *Acta Orthop Scand*, Vol. 59(1), 1988, pp. 19–23.

8 Esses, S. I., Lotz, J. C., and Hayes, W. C., "Biomechanical Properties of the Proximal Femur Determined in-vitro by Single-Energy Quantitative Computed Tomography," *J Bone Min Res*, Vol. 4, 1989, pp. 715–722.

9 Hayes, W. C., and Gerhart, T. N., "Biomechanics of Bone: Applications for Assessment of Bone Strength," *Bone and Mineral Research, Annual III*, ed., W. A. Peck, Amsterdam, Elsevier Science Publishers, 1985, pp. 259–294.

10 Hayes, W. C., Myers, E. R., Morris, J. N., Rejda, S. A., Gerhart, T. N., Yett, H. S., and Lipsitz, L. A., "Fall Biomechanics as Determinants of Osteoporotic Hip Fracture Risk," *Steenbock Symp on Osteoporosis*, June, 1989.

11 Holbrook, T. L., Grazier, K., Kelsey, J. L., and Stauffer, R. N., "The Frequency of Occurrence, Impact, and Cost of Selected Musculoskeletal Conditions in the United States," *American Academy of Orthopaedic Surgeons*, 1984.

12 Kelsey, J. L., and Hoffman, S., "Risk Factors for Hip Fracture," *New Engl J Med*, Vol. 316, 1987, pp. 404–406.

13 Leichter, I., Margulies, J. Y., Weinreb, A., Mizrahi, J., Robin, G. C.,

Conforty, B., Makin, M., and Bloch, B., "The Relationship Between Bone Density, Mineral Content, and Mechanical Strength in the Femoral Neck," *Clin Orthop Rel Res*, Vol. 163, 1982, pp. 272-281.
14 Lotz, J. C., and Hayes, W. C., "The Use of Quantitative Computed Tomography to Estimate Risk of Fracture of the Hip from Falls," *J Bone Joint Surg [Am]*, Vol. 72-A, 1990, pp. 689-700.
15 Mazess, R. B., "On Aging Bone Loss," *Clin Orthop Rel Res*, Vol. 165, 1982, pp. 239-252.
16 Melton, L. J., O'Fallon, W. M., and Riggs, B. L., "Secular Trends in the Incidence of Hip Fractures," *Calcif Tissue Int*, Vol. 41, 1987, pp. 57-64.
17 Melton, L. J., III, Kan, S. H., Wahner, H. W., and Riggs, B. L., "Lifetime Fracture Risk: An Approach to Hip Fracture Risk Assessment Based on Bone Mineral Density and Age," *J Clin Epidemiol*, Vol. 41, 1988, pp. 985-994.
18 Melton, L. J., III, and Riggs, B. L., "Hip Fracture: A Disease and an Accident," *Current Concepts of Bone Fragility*, eds., H. K. Uhthoff and E. Stahl, Berlin, Springer-Verlag, 1986, pp. 385-389.
19 Melton, L. J., III, and Riggs, B. L., "Epidemiology of Age-Related Fractures," *The Osteoporotic Syndrome: Detection, Prevention, and Treatment*, ed., L. V. Aviola, Orlando, Grune & Stratton, Inc., 1987, pp. 1-30.
20 Melton, L. J., III, Wahner, H. W., Richelson, L. S., O'Fallon, W. M., and Riggs, B. L., "Osteoporosis and the Risk of Hip Fracture," *Am J Epidemiol*, Vol. 124(2), 1986, pp. 254-261.
21 Nevitt, M. C., "Falls and Instability in the Elderly: Host and Behavioral Factors," background paper prepared for Surgeon General's Workshop on Health Promotion and Aging, Washington, D. C., 1987.
22 Nickens, H., "Intrinsic Factors in Falling Among the Elderly," *Arch Intern Med*, Vol. 145, 1985, pp. 1089-1093.
23 Radebaugh, T. S., Hadley, E., and Suzman, R., *Falls in the Elderly: Biologic and Behavioral Aspects*, Philadelphia, W. B. Saunders, 1985.
24 Riggs, B. L., and Melton, L. J., III, "Involutional Osteoporosis," *N Engl J Med*, Vol. 314, 1986, pp. 1676-1686.
25 Riggs, B. L., Wahner, H. W., Seeman, E., Offord, K. P., Dunn, W. L., Mazess, R. B., Johnson, K. A., and Melton, L. J., III, "Changes in Bone Mineral Density of the Proximal Femur and Spine with Aging. Differences Between the Postmenopausal and Senile Osteoporosis Syndromes," *J Clin Invest*, Vol. 70, 1982, pp. 716-723.
26 Sartoris, D. J., Sommer, F. G., Marcus, R., and Madvig, P., "Bone Mineral Density in the Femoral Neck: Quantitative Assessment Using Dual-Energy Projection Radiography," *Am J Roentgen*, Vol. 144, 1985, pp. 605-611.
27 Smith, L., "Hip Fracture: The Role of Muscle Contraction or Intrinsic Forces in the Causation of Fractures of the Femoral Neck," *J Bone Joint Surg*, Vol. 35-A, 1953, pp. 367-382.
28 Viano, D. C., "Biomedical Responses and Injuries in Blunt Lateral Impact," *Proceedings of the 33rd Stapp Car Crash Conference*, 1989, pp. 113-142.
29 von Gierke, H. E., and Goldman, D. E., "Effects of Shock and Vibration on Man," *Shock and Vibration Handbook*, ed., C. M. Harris, New York, McGraw-Hill, 1988, pp. 44.1-44.57.
30 Wicks, M., Garrett, R., Vernon-Roberts, B., and Fazzalari, N., "Absence of Metabolic Bone Disease in the Proximal Femur in Patients with Fracture of the Femoral Neck," *J Bone Joint Surg [Br]*, Vol. 64, 1982, pp. 319-322.
31 Ziegert, J. C., and Lewis, J. L., "In-vivo Mechanical Properties of Soft Tissue Covering Bony Prominences," ASME JOURNAL OF BIOMECHANICAL ENGINEERING, Vol. 100, 1978, pp. 194-201.

APPENDIX I

Pelvis Release Experiment Validation Test

One objective of the validation test was to verify that no element of the apparatus other than the mechanical properties of the test subject significantly affected pelvis release force records. Another objective was to verify that the forces occurring in high impact velocity collisions could be predicted accurately from the measured effective mass, stiffness, and damping of the test subject in zero initial velocity pelvis release experiments.

To perform the pelvis release validation test, a simple mechanical surrogate of the human body was placed in the pelvis release apparatus (Fig. 8). The mass of the pelvis and other moving body elements was represented by a central 32 kg iron mass (M). The springlike action of the spine and lower limbs was simulated by a 2 cm diameter PVC pipe of 1.5 m length (P). Finally, the compliance of the soft tissues overlying the hip and the compliance of the hip joint capsule and bones was represented by a parallel arrangement of two identical steel springs (S) placed between the central mass and the force platform.

An initial set of experiments involved measuring the response of the surrogate to zero initial velocity, low amplitude step changes in force as in the pelvis release experiments. Five measures of this type were taken at end loads of 170, 230, 270, and 310 N. In all tests, the preload was adjusted to be 150 N below the end load. As in the reduction of pelvis release data, an iterative procedure was used to find the values of ζ, ω_n, and m best describing the first cycle of ringing in the measured force record. However, since approximately zero damping existed between the central mass and the force plate (but a damping action was contributed by the side constraints and PVC pipe), the mass-spring-damper model used in reducing pelvis release data was modified as shown in the inset of Fig. 8. The appropriate equation of motion therefore was the same as Eq. (2), but the transmitted reaction force no longer contained a damping term and was given by

$$F = kx. \qquad (1.1)$$

A sample measure of the response of the surrogate in a simulated pelvis release experiment is shown in Fig. 9. In this trial, the preload was 66 N and the end load was 192 N. The theoretical prediction (broken curve) is in good agreement with the measured force (solid curve) when the parameters describing the experiment are $\omega_n = 62.9$ rad/s, $\zeta = 0.067$, and $m = 32$ kg. Corresponding values of k and b are 126 kN/m and 277 N-s/m, respectively. Additional tests revealed that k and b remained approximately constant when the end load was varied, averaging 123 ± 8 kN/m and 267 ± 54 N-s/m, respectively.

An additional set of experiments involved five repeated drops of the surrogate on the force platform from an initial height

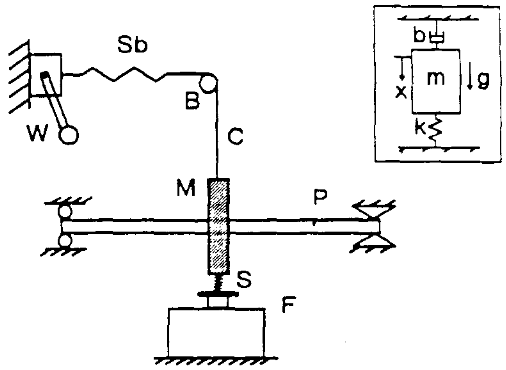

Fig. 8 Human body surrogate for validating the pelvis release experiments. A mass (M) is fixed at the center of a PVC pipe (P). A steep spring (S) is placed between the mass and the force plate. The chain (C), brake (B), bias spring (Sb), and winch (W) are used in pelvis release experiments.

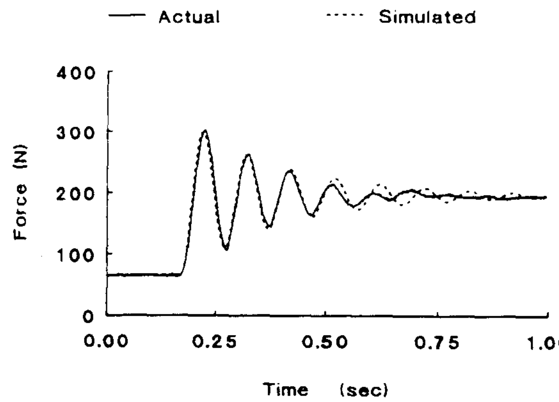

Fig. 9 Typical zero initial velocity test with the surrogate. The solid line shows the measured force, and the broken line shows the force calculated by Eq. (I.1) using $F_0 = 66$ N, $\omega_n = 62.9$ rad/s, and $\zeta = 0.067$.

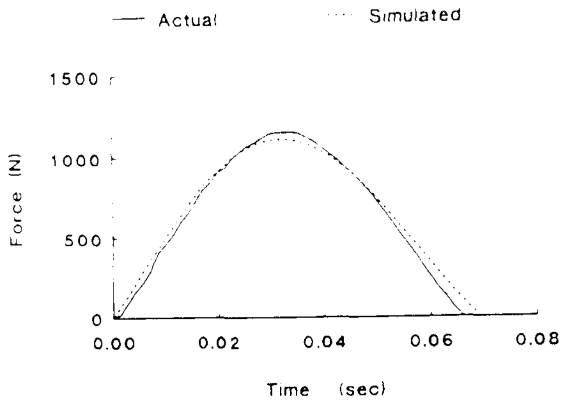

Fig. 10 Fall impact test with the human body surrogate. The solid line shows the force occurring in the first contact period when the surrogate is dropped from a height of 10 mm onto the force platform. The broken line shows the force predicted by Eq. (I.1) using $F_0 = 0.0$, $u = 0.53$ m/s, $\omega_n = 61.9$ rad/s, and $\zeta = 0.067$.

of 10 mm (the maximum height capable of being supported by the brake). The solid line in Fig. 10 shows the first contact period in a typical force record from these experiments. The peak force (1.15 kN) is over 3.1 times the mean peak force (and over 7.6 times the amplitude of force) observed in simulated pelvis release experiments (370 N). The impact velocity u was estimated at 0.53 m/s by equating the kinetic energy upon impact to the gravitational plus elastic potential energy (due to the deflection of the pipe) upon release. The resulting peak force of the broken curve (1.11 kN), calculated from Eq. (I.1) assuming $F_0 = F_S = 0$, $\omega_n = 61.9$ rad/s, and $\zeta = 0.067$, is within 4 percent of the actual peak force. Moreover, the predicted rise time to peak force (31.4 ms) is within 4.5 percent of the measured time (32.8 ms). Thus the pelvis release technique can provide good estimates of both the peak force and the rate of loading in nonzero initial velocity collisions.

Finally, to verify the accuracy of pelvis release measures of effective stiffness, we measured the force-deflection behavior of a single spring of the two spring combination in a servohydraulics materials test system (Model 1331, Instron Corp., Canton, MA). To compare the resulting spring constant (50.7 kN/m) to the value measured by the pelvis release technique, we first subtracted the measured stiffness of the PVC pipe (28 kN/m) from the mean effective stiffness measured in simulated pelvis release tests, and then divided the result in two (accounting for the two springs in parallel). The resulting value (47.5 kN/m) was in good agreement with the static measure. Considering the success of both this test and the impact test (described above), we feel that pelvis release experiments represent a simple yet accurate method for measuring the effective stiffness and damping that (together with the mass and impact velocity) govern the force applied to the hip in falls from standing height.

APPENDIX II

Determination of Force Platform Stiffness

To eliminate the effect of the force platform compliance on pelvis release measures of effective stiffness and damping, the stiffness of the force platform was measured in a force-deflection test and subtracted from pelvis release data. The test, which was conducted using an Instron servohydraulics testing machine over a range of force between 100 and 1000 N, revealed a force-dependent stiffness for the force platform that could be well represented by

$$K = 201956\, F^{0.113}, \tag{II.1}$$

where F is force in N, and K is stiffness in N/m.

Since this stiffness element was in series with the spring of the body, pelvis release data were adjusted as follows:

$$k_{\text{body}} = k_{\text{measured}} K / (K - k_{\text{measured}}), \tag{II.2}$$

$$\omega_{\text{body}} = (k_{\text{body}}/\text{m})^{1/2}, \tag{II.3}$$

$$b_{\text{body}} = 2\zeta\omega_{\text{body}}\text{m}. \tag{II.4}$$